



## Synthesis and Characterization of SnS: 3%Bi thin Films for Photovoltaic Applications

**Duaa Muneer Sadiq**

Department of physics, College of Education  
For Pure Science Ibn Al-Haitham,  
University of Baghdad, Baghdad, Iraq.  
[Doaa.Moneer1204a@ihcoedu.uobaghdad.edu.iq](mailto:Doaa.Moneer1204a@ihcoedu.uobaghdad.edu.iq)

**Bushra K.H. Al-Maiyaly**

Department of physics, College of Education  
For Pure Science Ibn Al-Haitham,  
University of Baghdad, Baghdad, Iraq.  
[boshra.k.h@ihcoedu.uobaghdad.edu.iq](mailto:boshra.k.h@ihcoedu.uobaghdad.edu.iq)

**Article history: Received 7 July 2022, Accepted 21 August 2022, Published in April 2023.**

[doi.org/10.30526/36.2.2930](https://doi.org/10.30526/36.2.2930)

### Abstract

In the present article, Nano crystalline SnS and SnS:3% Bi thin films were fabricated using thermal evaporation with  $400 \pm 20$  nm thickness at room temperature at a rate deposition rate of  $0.5 \pm 0.01$  nm/sec then annealing for one hour at 573 K for photovoltaic application. The prepared samples were characterized in order to investigate the structural, electrical, morphological, and optical properties using diverse techniques. XRD and SEM were recorded to investigate the effect of doping and annealing on structural and morphological possessions, respectively. XRD showed an SnS phase with polycrystalline and appeared to form an orthorhombic structure, with the distinguish trend along the (111) grade, varying crystallite size from (19.45-25.95) nm after doping and annealing. SEM investigations of these films show extremely fine nanostructures and demonstrated excellent adhesion, after Bi-doping, the nanostructures remained identical with a little change. UV/Visible studies were made in the range of wavelength (300-1100) nm to calculate the optical constants for these films. These measurements revealed a high value of the absorption coefficient and decrease the optical energy gap values from (1.85 -1.6) eV after doping with 3% Bi. The characterization of these films it can be chosen in the application of solar cells. On the other hand, the optical properties of SnS films have been enhanced by Bi-doping.

**Keywords:** SnS, doping, thermal evaporation, thin films.

### 1. Introduction

SnS (Tin sulfide) is the greatest promising IV–VI semiconductor for photovoltaic cells as absorber material. It has the best band gap (direct 1.3-1.7) eV, indirect 1.0-1.2 eV), robust absorption coefficient above  $10^4$  cm<sup>-1</sup> in the visible region range, simple phase configuration, safe, orthorhombic crystal structure, p-type conductivity, suitable for photodetector, and solar cell application [1-6]. Many types of research using diverse deposition techniques to manufacture Tin sulfide thin films, such as thermal evaporation [5,7], chemical deposition [6,8], spray pyrolysis [9], Electron beam evaporation [10], radio frequency(RF)magnetron sputtering [11], atomic layer deposition [12,13]. The effect of various dopant material on SnS properties thin film were

examined by different researchers for example, electrochemical deposition method was used to prepare SnS thin film Nanostructured pure and doped-In deposited on (FTO) substrates, and energy gap (Eg) decreased after doping. All films were p-type conductivity[14]. The plasma vapor method was used to fabricate SnS<sub>2</sub>/SnS Heterojunction diode [15], and (p-SnS/n-CdS:In) was prepared by spray pyrolysis for solar cell application, 1.3% efficiency was obtained, (0 to 6 at wt. %) concentrations of Al doping with spray pyrolysis, the optical energy gap decreased (1.97 to 1.72) eV. All films were doped and pure showed p-type conducting with efficiency of 0.093%, which evaluated for 4% Al[16]. The thermal evaporation method was used to deposit SnS thin film for solar cells with 1.6% efficiency [4] SnS: Bi(between 0 and 8 at%) prepared by spray pyrolysis at substrate temperature 350 °C. The value of energy gap decreased from 1.6 eV to 1.4 eV, low resistivity of  $4.788 \times 10^{-1} \Omega\text{-cm}$  and higher carrier concentration of  $3.625 \times 10^{18} \text{ cm}^{-3}$  was obtained for SnS:Bi (6 at%)[ 17]. The chemical deposition was used to deposit SnS thin films with F-doped, the energy gap decreased from 1.7 eV to 1.1 eV, a solar cell with 0.96% efficiency fabricated with CdS as window layers [18]. Ag-doped SnS thin films on glass substrate using spray pyrolysis at 400 °C with (1, 2, and 3)%, when increased concentration doping the energy gap, grain size, and carrier concentration decreased, n-type conductivity showed by Hall Effect [19]. The influence of Cu doping was studied by different researchers [20-22], SnS with Cu 5% film was deposited by PLD (pulsed laser deposition), the energy gap was direct with 2.23 eV, and the absorption coefficient was  $105 \text{ cm}^{-1}$  [20]. SnS: Cu (up to 10 at. %) prepared by spray pyrolysis, the lowest resistivity, and upper carrier concentration was gained in thin films at 8 % Cu [21]. (1, 3, and 5)% of Cu: SnS films were prepared by using thermal evaporation, with the roughness, grain size, and absorption coefficients increasing while the energy gap decreased after doping, with 3.5% efficiency for p-SnS: Cu/n-Si solar cell [22].

This work aims to pay attention to the effect of (3% Bi) dopant and thermal annealing at 300 °C with (3% Bi) on SnS thin film properties by using the thermal evaporating technique. The correlation between the morphological, structural, and optical characteristics of SnS thin films was investigated.

## 2. Experimental

SnS thin films pure and Bi-doped (SnS: 3% Bi ) have been deposited by thermal evaporation technique using Edward coating unit on glass substrates under high vacuum of ( $3 \times 10^{-6}$ ) torr of 400 nm thicknesses at R.T and annealing at 573K for 1 hour. These films were synthesized after preparation of SnS alloy by mixing (Sn) & (S) elements with high purity (99.99%) in (1:1) ratio, put in a quartz tube evacuated at pressure ( $4 \times 10^{-4}$  m-bar), then heated in an electric oven at 1273 K for 5 hours, finally left to cool gradually. Films thickness t was determined by the weight method. X-ray diffraction technique was used to examine the structure of the alloy and all films prepared with ( $\lambda = 1.5418 \text{ \AA}$ ), 40 kV voltage, and 20 mA current using CuK $\alpha$  radiation. Scherer's Formula was used to calculate the crystallite size [23, 24]:

$$C.S = \frac{0.94\lambda}{\beta \cos\theta} \quad (1)$$

Where  $\lambda$ : denotes the XRD wave length,  $\beta$ : denotes the FWHM of the peaks, and  $\theta$ : denotes Bragg's angle.

Williamson and Smallman's equation was used to calculate the dislocation density ( $\delta$ ) [24]:

$$\delta = \frac{1}{(C.S)^2} \quad (2)$$

Morphology of the surface of films prepared were determined by SEM. Transmission spectrum has been recorded to investigate the optical properties in the range (300-1100) nm. Tauc's equation was used to calculate the optical energy gap: [25, 26]

$$(\alpha h\nu) = A(h\nu - E_g)^n \quad (3)$$

Where A: is constant and n is a number depending on the transition type.

The refractive index values can be calculated in the formula: [27]

$$n = \{[4R / (R-1)] - K^2\}^{1/2} - [(R+1) / (R-1)] \quad (4)$$

Where R is the reflectance which calculated by using equation:

$$R = 1 - T - A \quad (5)$$

The extinction coefficient (K) is calculated by: [28]

$$\alpha = 4\pi K / \lambda \quad (6)$$

### 3. Results and Discussions

#### 3.1. X-ray Diffraction Analyses

The principal X-ray diffraction peaks for SnS alloy were shown in Figure 1. The results showed polycrystalline, a predominant orthorhombic SnS (111) development plane at  $2\theta = 31.53^\circ$  were found to be in good agreement with the standards (ICDD card No.00-039-0354). Structural Oparameters for SnS alloy were shown in **Table (1)**, such as crystalline size, lattice constants, and planar spacing (d). Figure 2 showed XRD patterns for non-doped, Bi-doped SnS films with Bi concentrations of 3 % and films doped with annealing at 573 K. All thin films showed polycrystalline, structure, and the peak positions of the films were found to be in good agreement with the standards card, and with a preferential orientation at the location of  $2\theta = 31.53^\circ$ . No peaks corresponding to the Bi phase were observed. In addition, the peak positions changed marginally after doping. This demonstrated that Bi ions moved to retinal sites to replace Sn ions supported by the fact that the ionic radius at doped is (90) was less than the host (96). **Table (2)** contains all the values for SnS films.

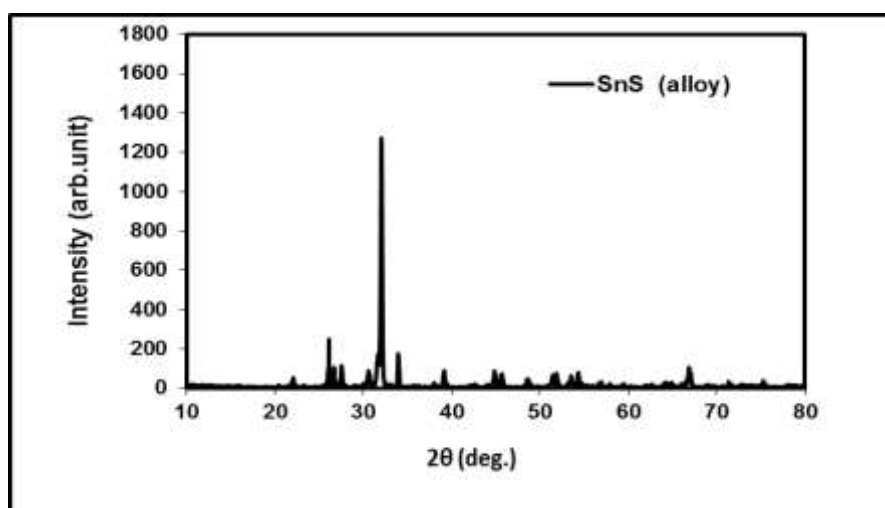


**Figure 1.** XRD of Tin sulfide alloy

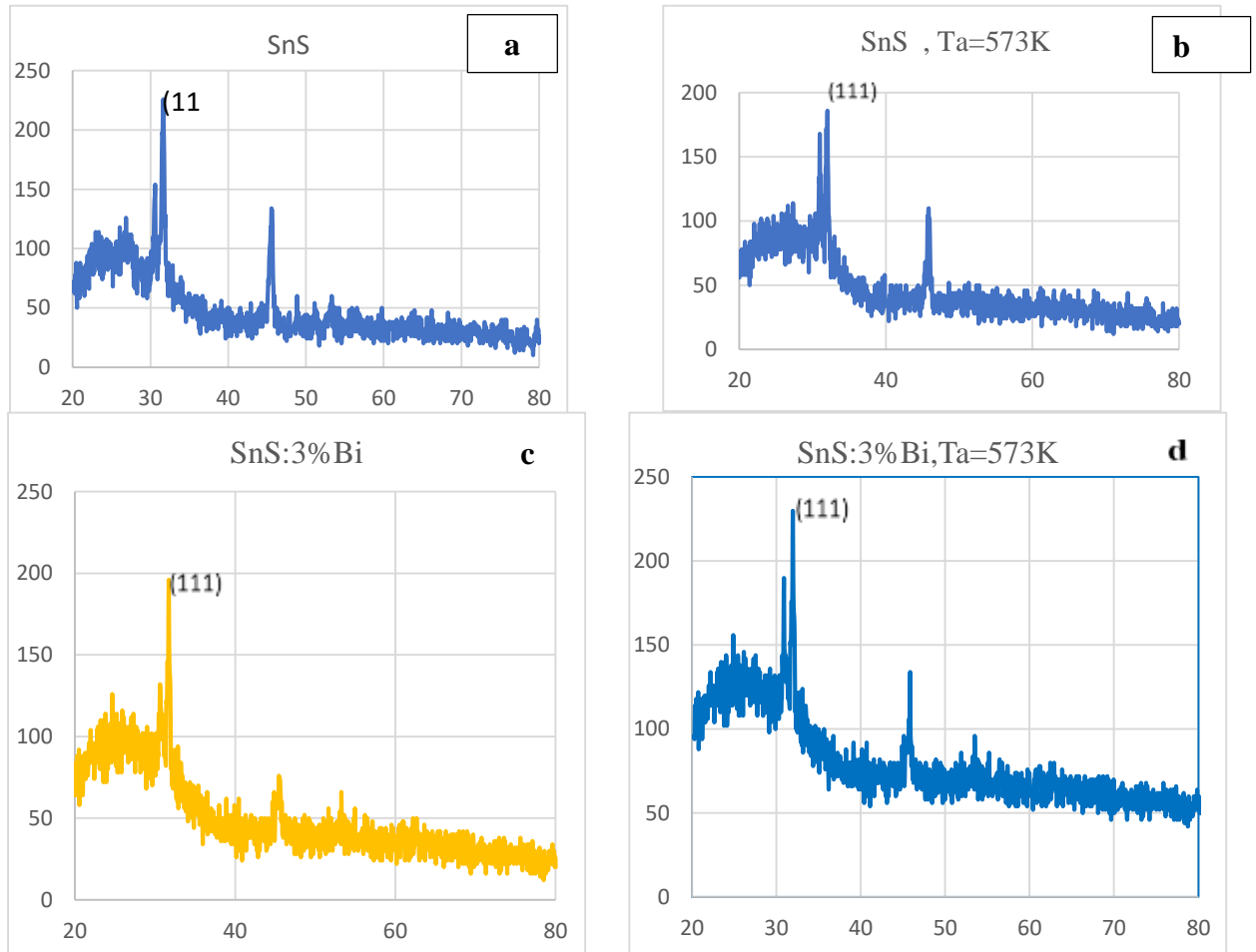


**Figure 2.** XRD of Tin sulfide thin films a) pure b) pure at Ta=573 K c) doped 3% Bi d) doped 3% Bi at (Ta=573 K)

**Table 1.** Structural parameters for Tin sulfide alloy.

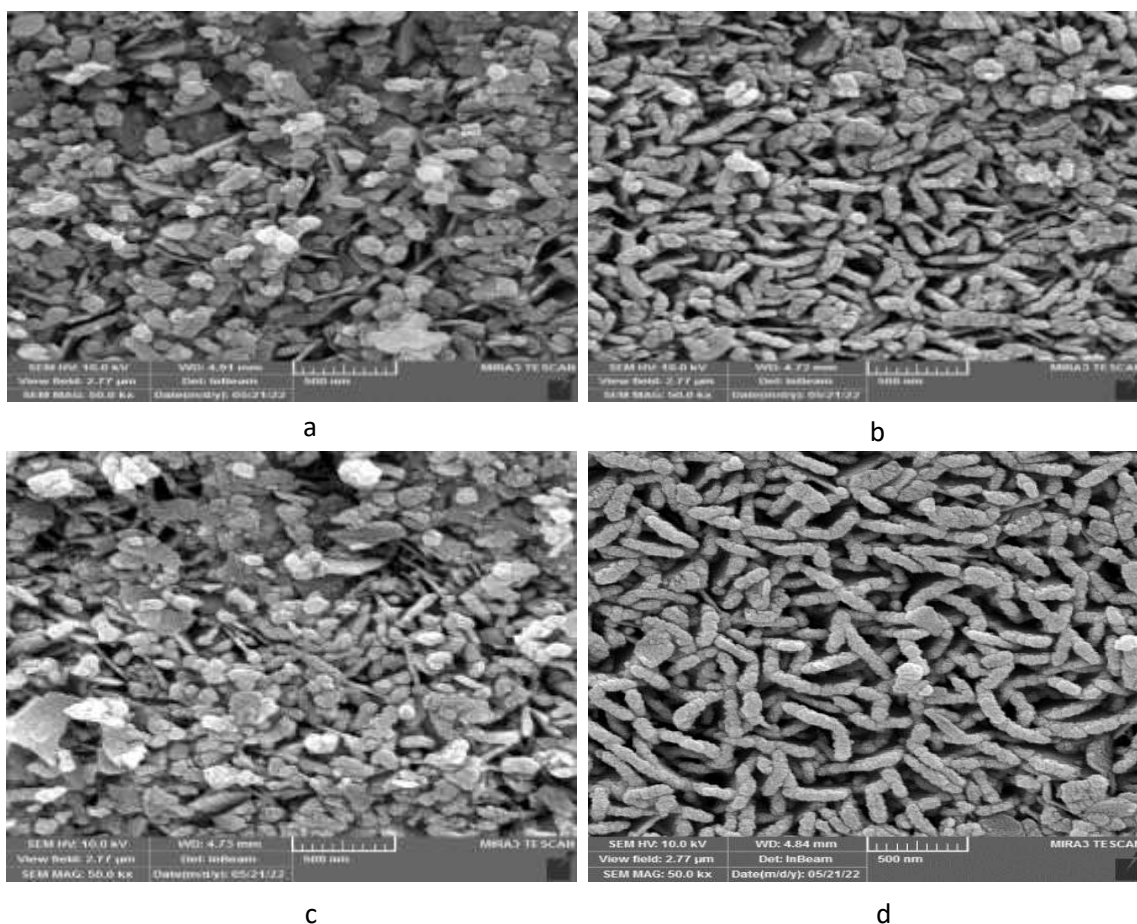
2θ (Std.) (Deg.)	2θ (Exp.) (Deg.)	d(Std) (Å)	d(Exp) (Å)	hkl	FWHM (Deg.)	c.s(nm)	a(Std.) (Å)	a(Exp.) (Å)
22.0106	22.0764	4.035000	4.02322	110			4.3291	4.3321
26.0094	26.0873	3.423000	3.41304	120				
27.4719	27.5639	3.244000	3.23346	021				
30.4731	30.6213	2.931000	2.91722	101				
31.5313	31.6613	2.835000	2.82373	111	0.16830	51.255		

Table 2. Structural parameters for SnS.

Sample		2 $\theta$ (Deg.)	FWHM(Deg.)	d <sub>hkl</sub> (exp)	C.S (nm)	$\delta * 10^{15}$ (lines/m <sup>2</sup> )
SnS		31.708	0.4039	2.81966	19.457	2.641486
		30.6853	0.4857	2.91129	17.73825	3.178179
SnS	573	29.344	0.2	3.04122	42.94238	0.542285
		33.0873	0.445	2.705	19.47689	2.636093
SnS:3%B		31.6286	0.4144	2.8265	20.838	2.302969
		30.5689	0.3373	2.922	25.53535	1.533615
SnS:3%B	573	31.9743	0.333	2.7968	25.95402	1.484536

### 3.2. (SEM) Measurement

The most widely used technique for nanomaterial and nanostructure characterization was SEM because of its great nanometer resolution. SEM images of SnS and SnS :3% Bi before and after annealing at 573 K thin films produced on a glass substrate were used to investigate the shape of the surfaces of the samples. All samples have extremely fine nanostructures, as shown in **Figure 3**. The surface of nanostructure seems to be covered with much small nano grain in the image showing the SEM cross-sectional image of a film that has been laid in an irregular pattern. The SnS films, on the other hand, demonstrated excellent adhesion the shapes of the nanostructures remained identical with a little change after Bi-doping was added as well as the image shows that after annealing the particles became fused.



**Figure 3.** SEM images of SnS thin films, **a)** pure at R.T, **b)** pure at  $T_a=573$  K, **c)** doped 3% Bi at R.T **d)** doped 3% Bi at ( $T_a=573$  K)

### 3.3. Optical Measurement

**Figure (4)** displays the optical absorbance range of SnS and SnS: 3% Bi thin films before and after annealing at 573 K. This figure shows the increasing absorbance after doping, while the transmittance of the films decreased. This means the presence of Bi ions in the composition of SnS will contribute to this pattern of transmittance spectrum, as well as size differences, and the packing of crystallites. This behavior is similar to the study [14] and [22] when doped with In and Cu, respectively. The improvement in absorbance might be attributed to a reduction in optical scattering. Also, notice a high absorbance value at range (400-600) nm. These films have high absorption coefficients ( $\alpha > 10^4 \text{ cm}^{-1}$ ), and increase after doping, as shown in **Figure (5)**. The results show that doped with 3% Bi results in a decrease in the band gap from 1.85 eV to 1.6 eV shifting to longer wavelength NIR (near infrared ray) areas, as shown in **Figure (6)**. It shows the relation  $(\alpha h\nu)^2$  with  $h\nu$  for SnS thin films according to Tauc's equation. This behavior can be attributed to the fact that the doping atom creates levels inside the energy band due to decreased energy gap value. This result agrees with ref. (17). The value of the energy gap of these films was displayed in **Figure (7)**, which would be better matched with solar cell application. The increase of energy gap after annealing due to decrease tails and the density of localized states in the films due to increasing in stoichiometric composition which leads to an increase in the band gap, as well

as the increases in crystallite size and the grain boundaries after annealing, might also lead to the increase in the optical band gap.

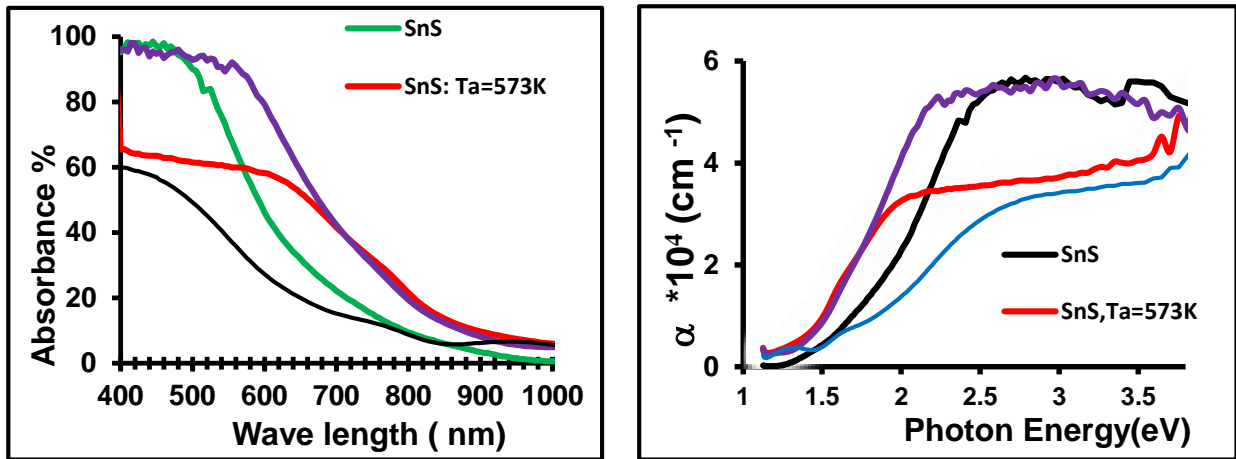


Figure 4. Absorbance of SnS thin films Figure 5 shows the relationship between the absorption versus wavelength coefficient and photon energy for SnS thin films.

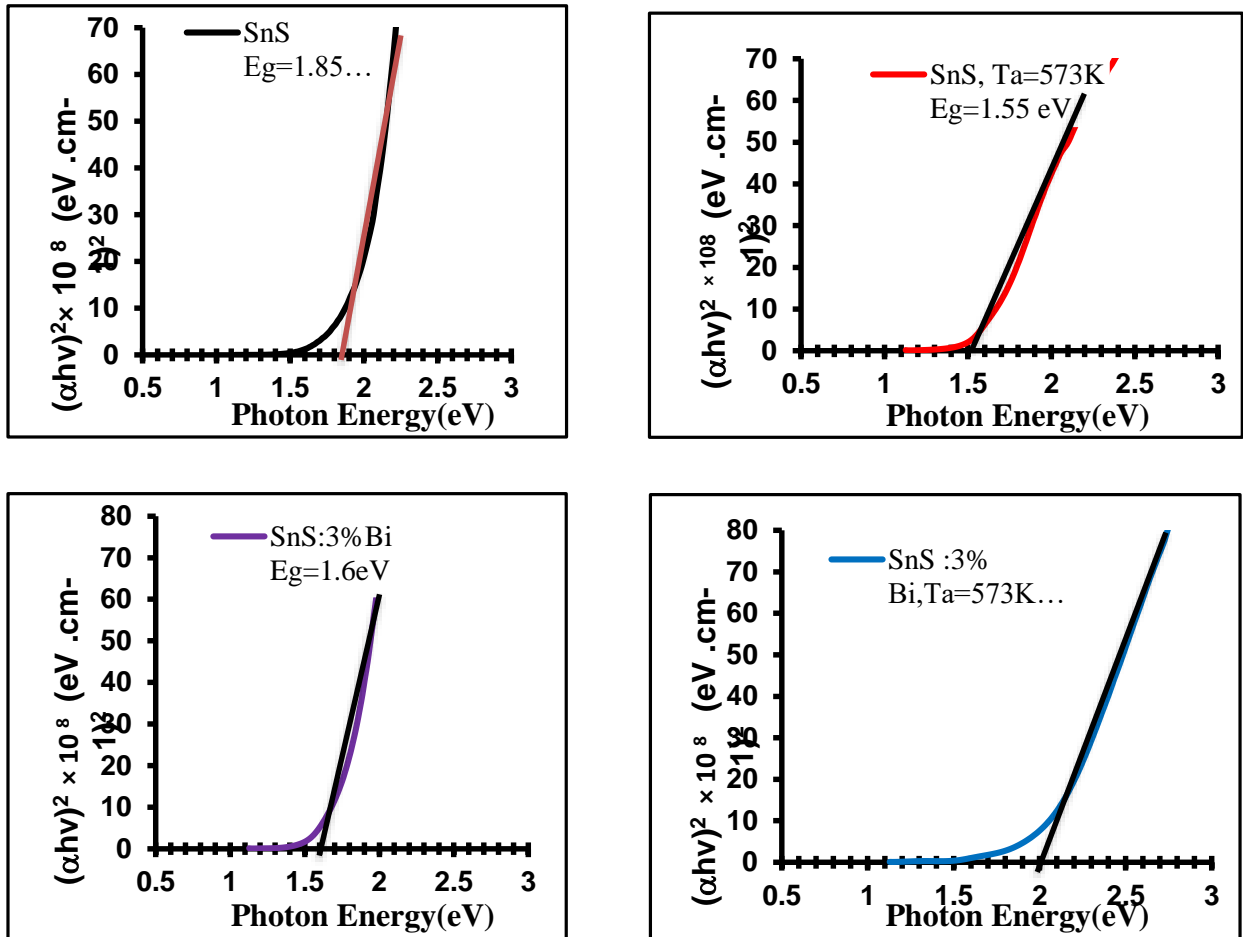


Figure 6. shows the relationship between  $(\alpha h\nu)^2$  and photon energy in SnS thin films a) pure at R.T, b) pure at R.T, c) doped 3% Bi(SnS:Bi )at (273K), d) doped 3% Bi at (Ta=573 K)



Figure 7. Optical energy gap for Tin sulfide films

The behavior of refractive index ( $n$ ) versus photon energy for (SnS and SnS:3%Bi before and after annealing at  $T_a=573$  K) films is shown in **Figure (8)**. This figure shows that refractive index values change after doping and annealing due to changes in the structural characteristics of films and decrease at higher photon energies .

**Figure (9)** explains the variation of the extinction coefficient ( $K$ ) with  $h\nu$  for SnS thin films pure and doped 3% Bi before and after annealing at ( $T_a=573$  K). The extinction coefficient values increase after doping and annealing. The behavior of the extinction coefficient values is similar to that of the absorption coefficients for all ranges of the wavelength spectrum.

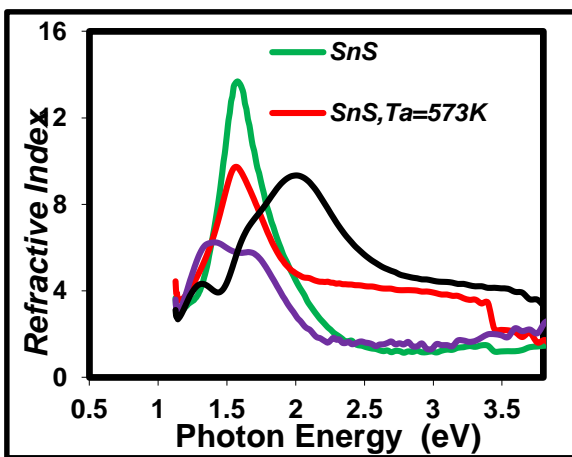


Figure 8. Refractive index versus  $h\nu$  for SnS thin films

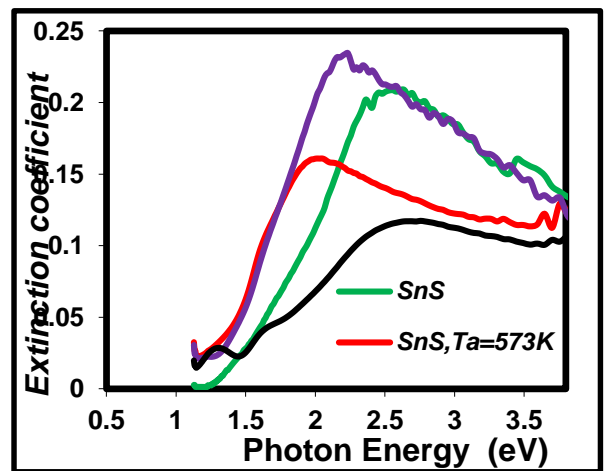


Figure 9. Extinction coefficient versus  $h\nu$  for SnS thin films



Table 3. SnS thin films optical constants

State	$E_{g}^{opt}$ (eV)	Optical parameter at $\lambda = 500$ nm				
		$\alpha \times 10^4$ $cm^{-1}$	n	K	$\epsilon_1$	$\epsilon_2$
SnS	1.85	5.179	1.461	0.20618	2.094	0.602
SnS Ta =573K	1.55	3.54	4.242	0.1409	17.97	1.195
SnS : 3% Bi	1.6	5.344	1.667	0.212	2.736	0.7096
SnS : 3% Biat Ta =573K	2	2.834	5.77	0.1128	33.37	1.304

#### 4. Conclusion

Pure Tin sulfide and 3% Bi doped thin films before and after annealing at 573 K were grown with 400 nm thickness by thermal evaporation technique. The effects of 3% Bi doping on structural, morphology, optical, and electrical of SnS thin films were investigated.

The XRD patterns for pure and doped SnS nanostructured thin film displayed polycrystalline orthorhombic structure with preferential orientation in (111) direction. It was observed that Bi incorporation in the structure of SnS played an important role in the crystallite size, which increased from 19.45 to 25.95 nm. From SEM, Nano structure for pure SnS and doping with Bi were found with a gradual change in morphology. UV-visible analysis showed all samples have a strong transition in the visible region with a direct optical energy gap which decreased from 1.85 eV to 1.6 eV. It was observed that Bi doping and annealing at 573 K for one hour have an effect on energy bands. All optical constants depended on doping and annealing. The optical performance of Tin sulfide films were improved due to Bi-doping indicating that these films were good for photovoltaic application.

#### References

1. Kawano, Y.; Chantana, J.; Minemoto, T. Impact of growth temperature on the properties of SnS film prepared by thermal evaporation and its photovoltaic performance, *Curr. Appl. Phys.*, **2015**, *15*, 897–901
2. Schneikart, A.; Schimper, H. J.; Klein, A.; Jaegermann, W. Efficiency limitations of thermally evaporated thin-film SnS solar cells, *J. Phys. D Appl. Phys.* **2013**, *46*, 305109.
3. Vidal. J.; Lany. S.; D’Avezac. M.; Zunger. A.; Zakutayev. A.; Francis, Band structure, optical and defect physics of photovoltaic semiconductor SnS, *J. Appl. Phys. Lett.*, **2012**, *100*, 032104.
4. Steinmann, V.; Jaramillo, R.; Hartman, K.; Chakraborty, R.; Brandt, R. E.; Poindexter, J. R.; 3.88% Efficient Tin Sulfide Solar Cells using Congruent Thermal Evaporation, *Adv. Mater.*, **2014**, *26*, 7488–7492.
5. Balakart, H. R.; Santhanam, A.; Aslam, K.; A. M.; El-Toni, A. A.; Ansari, A. I.; Mohd, S. S. A.; Performance analysis of SnS thin films fabricated using thermal evaporation technique for photodetector applications, *Optik*, **2021**, *244*, 167460.

6. Rohini, N.; Mohan, O. G.; Daza, A. Rosa, G. A.; ALizabeth, E.; Santana, A.; Beristain, M. T.; Nair, P. K. Thin films of p-SnS and n-Sn<sub>2</sub>S<sub>3</sub> for solar cells produced by thermal processing of chemically deposited SnS, *Journal of Alloys and Compounds*, **2022**, 892, 5, 162036.
7. Hasan, B. A. Dielectric Properties of Vacuum Evaporated SnS Thin Films. *Int. J. Nanotechnol. Adv. Mater.*, **2013**, 1, 87–93.
8. Gode, F.; Guneri, E.; Baglayan. O. Effect of tri-sodium citrate concentration on structural, Optical and electrical properties of chemically deposited tin sulfide films. *Appl. Surf. Sci.* **2014**, 318, 227–233.
9. Messaoudi, M.; Aida, M. S.; Attaf, N.; Bezzi, T.; Bougdira, J.; Medjahdi, G. Deposition of tin(II) sulfide thin films by ultrasonic spray pyrolysis: Evidence of sulfur exo-diffusion., *Mater. Sci. Semicond. Process.* **2014**, 17, 38–42.
10. Tanuševski, A.; Poelman, D. Optical and photoconductive properties of SnS thin films prepared by electron beam evaporation, *Sol. Energy Mater. Sol. Cells*, **2003**, 80, 297–303.
11. Sousa, M. G.; Da Cunha, A. F.; Fernandes, P. A. Annealing of RF-magnetron sputtered SnS<sub>2</sub> precursors as a new route for single phase SnS thin films. *J. Alloys Compd.*, **2014**, 592, 80–85.
12. Sinsermsuksakul, P.; Heo, J.; Noh, W.; Hock, A. S.; Gordon. R. G. Atomic Layer Deposition of Tin Monosulfide Thin Films. *Adv. Energy Mater.*, **2011**, 1, 1116–1125.
13. Kim, J. Y.; George. S. M. Tin Monosulfide Thin Films Grown by Atomic Layer Deposition Using Tin 2, 4-Pentanedionate and Hydrogen Sulfide, *J. Phys. Chem.*, **2010**, 114, 17597–17603.
14. Hosein, K. Optoelectronic properties of In-doped SnS thin films, *Ceramics International*, **2019**, 45, 1, 334-345.
15. Sánchez-Juárez, A.; Tiburcio-Silver, A.; Ortiz, A. Fabrication of SnS<sub>2</sub>/Sn Sheterojunction thin film diodes by plasma-enhanced chemical vapor deposition, *Thin Solid Films*, **2005**, 480, 4, 452–456.
16. Sebastian, S.; Kulandaisamy, I.; Arulanantham, M. S.; Valanarasu, S.; Kathalingam, A.; JesuJebathew, A.; Mohd, S.; Karunakaran, M. Influence of Al doping concentration on the opto-electronic chattels of SnS thin films readied by NSP, *Optical and Quantum Electronics*, **2019**, 51, 100, 1-16.
17. Gowri, M. A.; Dhanapandian, S.; Chellasamy, M.; Thaiyan, M. Effect of doping concentration on the properties of bismuth doped tin sulfide thin films prepared by spray pyrolysis, *Materials Science in Semiconductor Processing*, **2014**, 17, 138–142.
18. Victoria, E.; González-Flores, R.; Neendoor, M. R. Ballinas-Morales, M. T.; Nair, S.; Thin film solar cells of chemically deposited SnS of cubic and orthorhombic structures, *Thin Solid Films*, **2019**, 672, 62-65.
19. Fadavieslam, M. R. Effect of Ag doping on physical properties of tin-sulfide thin films for optoelectronic applications prepared by spray pyrolysis, *Applied Physics*, **2018**, 124, 9.
20. Liu, L.; Yu. L.; Li, X. L.; Wang, Z.; Liang, Q. Structure and Optical Properties of Cu-doped SnS Thin Films Prepared by PLD, *Chinese Journal of Luminescence*, **2015**, 36, 11, 1311-1319.
21. Santhosh, K.; Kumar, A.; Gowri, M.; Chaogang, L.; Mahalingam, T.; Dhanapandian, S. Influence of Cu dopant on the optical and electrical properties of pray deposited tin sulphide thin films, *Vacuum*, **2016**, 128, 226-229.

- 22.** Hanan, K. H.; Bushra, H. H.; Bushra, K. H.; Auday, H. S. Influence of Cu Dopant on SnS Thin Films Characterization and Enhance Efficiency of p-SnS:Cu /n-Si Solar Cell, *Key Engineering Materials*, **2021**,886, 66-74.
- 23.** Khudayer, I. H.; Hussien, B.H. Study of Some Structural and Optical Properties of AgAlSe<sub>2</sub> Thin Films, *Ibn Al-Haitham J. for Pure & Appl. Sci.*, **2016**,29 , 2, 41-51.
- 24.** Ghuzlan, S. A.; Bushra, K. H.; Al-Maiyaly Annealing effect on characterization of nano crystalline SnSe thin films prepared by thermal evaporation, *AIP Conference Proceedings*,**2019**, 2123, 020074.
- 25.** Bushra, H. H.; Hanan, K. H. Comparative Study for Optoelectronic Properties of Zn (Te, Se) Solar Cells, *NeuroQuantology*, **2020**,18, 5, 77.
- 26.** Bushra, K. H. AL-Maiyal; Bushra, H. H.; Hanan, K. H. GROWTH AND OPTOELECTRONIC PROPERTIES OF p-CuO:Al/n-Si HETEROJUNCTION, *Journal of Ovonic Research*, **2020**, 16, 5.
- 27.** Bushra, K. H. AL-Maiyal Study the Effect of Thickness on the Electrical Conductivity and Optical Constant of Co<sub>3</sub>O<sub>4</sub> Thin Films, *Ibn Al-Haitham J. for Pure & Appl. Sci*, **2013**, 26, 1.
- 28.** Bushra, K. H. AL-Maiyal The Influence of Annealing and Doping by Copper on Electrical Conductivity of CdTe Thin Films, *Ibn Al-Haitham J. for Pure & Appl. Sci*, **2015**, 28, 3.